PHYSICAL REVIEW A VOLUME 26, NUMBER 6 DECEMBER 1982

Picosecond studies of energy transfer of donor and acceptor dye molecules in solution

P. Y. Lu, Z. X. Yu,* R. R. Alfano, and J. I. Gersten
Picosecond Laser and Spectroscopy Laboratory, Physics Department,
The City College of the City University of New York, New York, New York 10031
(Received 21 August 1981)

The fluorescence temporal profiles for donor and acceptor molecules in the binary mixtures of (1) rhodamine 6*G* and oxazine-4-perchlorate and (2) rhodamine *B* and nile-blue-*A*-perchlorate were measured using a 6-ps laser pulse and streak camera-video system. The theoretical calculations were fitted to the experimental data to obtain fundamental information concerning energy-transfer dynamics in binary mixtures.

I. INTRODUCTION

The study of the transfer of energy between donor and acceptor dye molecules in solution has both theoretical and practical importance. Dyes play a major role in various fields. They are commonly used as biological and industrial stains. In photosynthesis, dyes transfer optical energy from one spectral region to another. Dyes can increase the efficiency in solar energy conversion by absorbing energy in a wide spectral region. It is important to understand the mechanisms for energy losses and transfer in neat and binary dye mixture in solution. A series of experiments[1–11] on dye mixtures have shown that the excitation energy may be efficiently transferred from a photoexcited molecule (the donor) to an unexcited molecule (the acceptor). Dye lasers have been widely used in spectroscopic systems for photophysics and photochemistry studies. Energy transfer from an absorber (donor) molecule to an acceptor molecule in a dye laser mixture affects the operation and spectral output of the dye laser. The mixture of two dissimilar dye molecules, for example, rhodamine 6*G* and cresyl violet, can increase the efficiency of a dye laser of cresyl violet. Lin and Dienes[5] have studied the excitation transfer in a laser dye mixture of rhodamine 6*G* and cresyl violet by studying the fluorescence kinetics of only the donor molecule. They found a Stern-Volmer quenching relation for the donor system. Rehm and Eisenthal[4] also studied the donor kinetics and found that the energy transfer between the rhodamine 6*G* (the donor) and malachite green (the acceptor) is in agreement with the Forster theory. Recently, Porter and Tredwell[11] studied the same system of rhodamine 6*G* and malachite green and obtained a value of $R_0 = 52.5\ \text{Å} \pm 0.5\ \text{Å}$ for the Förster mechanism. However, these investigators have only studied the kinetics of the *donor system* to obtain information on the energy-transfer rates to the acceptor. These measurements do not give a complete picture of energy transfer to the acceptor because of competing nonradiative and radiative rates and concentration quenching from the donor and acceptor, spatial distribution, etc. It is essential to measure the *kinetics* of *both* the *donor* and *acceptor* molecules to obtain a complete description of the energy-transfer mechanism operating in the binary components of dyes in a solution.

In this paper, we present experimental measurements and theoretical calculations for the energy-transfer dynamics in two mixtures composed of (1) rhodamine 6*G* (the donor) and oxazine-4-perchlorate (the acceptor), and (2) rhodamine *B* (the donor) and nile-blue-*A*-perchlorate (the acceptor). The fluorescence kinetics for neat dyes and for both the donor and acceptor dyes in the binary mixture were investigated at concentration $2.5 \times 10^{-3} M$ in ethylene glycol at room temperature. The absorption and fluorescence spectra for the donors and acceptors used in the paper are displayed in Fig. 1.

II. THEORY

The long-range resonance energy-transfer rate between two species of molecules was shown by Forster to depend on distance as R^{-6} due to the dipole-dipole[12–15] interaction. Dexter[16] extended this theory and included exchange and higher multipole interaction in the study of energy transfer. Yokota and Tanimoto[17] developed a model treating the diffusion of the excited molecule as a perturbation to the theory of long-range transfer. Later,

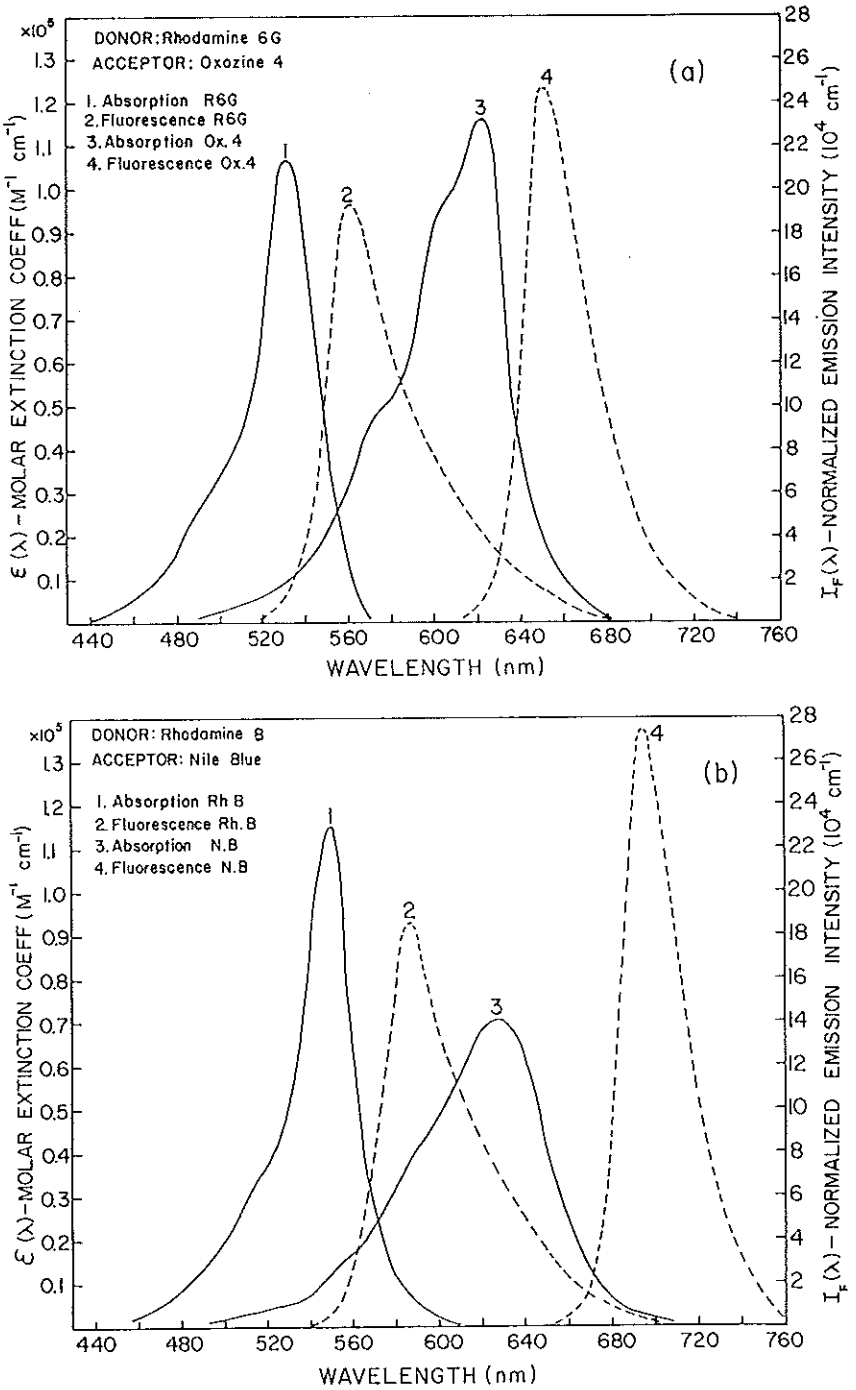

FIG. 1. Steady-state absorption and fluorescence spectra for donor and acceptor dye molecules. (a) R6G(*D*)-OX(*A*) and (b) RB(*D*)-NB(*A*).

Klein *et al.*[18] formulated the theory considering the diffusion effect and long-range energy transfer. Recently, Auerbach *et al.*[19] have considered a diffusion modulated donor-acceptor energy transfer in a disordered system and obtained the result that the fastest acceptor rise times occur in the limit of the slowest donor diffusion, and faster rise times also result from shortening of the range of the donor-acceptor transfer interaction. Furthermore, Allinger and Blumen[20] used statistics to investigate the direct energy transfer in the donor-acceptor system. Most of the theories and measurements emphasized the results of the donor in the energy-transfer process. There is lack of a concise theory

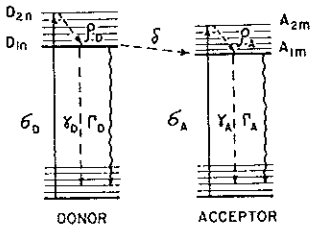

FIG. 2. Energy diagram for the theoretical model for the resonance energy transfer in the binary mixture solution. D_{1n} is the excited electronic state of the nth donor molecule. D_{2n} is the vibronic state associated with D_{1n}. Similarly, A is used for acceptor, and δ is the transfer rate.

which will fit the experimental results for the kinetics of *both* the *donor* and *acceptor*.

A theoretical model including the spatial distributions of the molecules and relaxation rates which accounts for the decay and rise-time fluorescence kinetics of both the donor and acceptor molecule is derived in this section. The energy-level diagram for the donor and acceptor are shown in Fig. 2. The rate equations describing the energy dynamics for photoexcited donor (D) and acceptor (A) molecules are as follows.

The donors are photoexcited to a vibrational state, denoted by S_1^* in the electronic manifold:

$$\dot{D}_{2n}+\rho_D D_{2n}=\sigma_D I_0\delta(t)\ . \tag{1}$$

Likewise, some acceptors are photoexcited to vibrational states S_1^* of the electronic manifold:

$$\dot{A}_{2n}+\rho_A A_{2n}=\sigma_A I_0\delta(t)\ . \tag{2}$$

The population of excited donor and acceptor molecules are described by equations

$$\dot{D}_{1n}+(\gamma_D+\Gamma_D)D_{1n}=\rho_D D_{2n}-\sum_m^{N_A}\delta_{nm}D_{1n} \tag{3}$$

and

$$\dot{A}_{1n}+(\gamma_A+\Gamma_A)A_{1n}=\rho_A A_{2n}+\sum_m^{N_D}\delta_{mn}D_{1m}\ , \tag{4}$$

respectively.

The following is a list of the symbols:

$I_0\delta(t)$ = ultrashort laser pulse (photons/cm^2 sec);

D_{jn} = probability for the nth donor molecule to be in the jth excited state;

A_{jn} = probability for the nth acceptor molecule to be in the jth excited state;

ρ_D = excited-state vibrational relaxation rate of donor molecule;

ρ_A = excited-state vibrational relaxation rate of acceptor molecule;

σ_A,σ_D = absorption cross sections in the acceptor and donor molecules;

γ_D = nonradiative decay rate of donor molecule;

γ_A = nonradiative decay rate of acceptor molecule;

Γ_D = radiative decay rate of donor molecule;

Γ_A = radiative decay rate of acceptor molecule;

δ_{nm} = transfer rate from the nth donor to mth acceptor;

$=1/\tau_D(R_0/R)^6$;

τ_D = fluorescence lifetime of donor;

and R_0 = the distance for which the rate of energy transfer is equal to the sum of all other donor deactivation rates.

In the case of xanthane and oxazine dyes in viscous liquids, the diffusion constants are on the order of 10^{-6} cm^2 sec^{-1} and the fluorescence lifetimes are on the order of 1 ns in the neat solution. In this case the diffusion length is about 3 Å. So the diffusion effect[18] is less important than the long-range energy mechanism and has been neglected here.

The initial conditions at $t=0$ for donor and acceptor probabilities are

$$D_{2n}(0^+)=\sigma_D I_0\ , \tag{5}$$

$$A_{2n}(0^+)=\sigma_A I_0\ , \tag{6}$$

$$D_{1n}(0^+)=0\ , \tag{7}$$

and

$$A_{1n}(0^+)=0\ . \tag{8}$$

Averaging over the spatial distribution of molecules is essential to describe the observed donor and acceptor kinetics. The equations for the fluorescence per unit volume $\mathscr{D}(t)$ and $\mathscr{A}(t)$ for the donor and acceptor molecules will follow. For the donors

$$\mathscr{D}(t)=\frac{1}{V}\left\langle\Gamma_D\sum_{n=1}^{N_D}D_{1n}\right\rangle=\frac{\Gamma_D}{V}\prod_{k=1}^{N_A}\left[\frac{1}{V}\int d\gamma_k 4\pi\gamma_k^2\right]\sum_{n=1}^{N_D}D_{1n}$$

$$=\frac{\Gamma_D}{V}\prod_{k=1}^{N_A}\left[\frac{1}{V}\int d\gamma_k 4\pi\gamma_k^2\right]\sum_{n=1}^{N_D}\int_0^t dt'\rho_D\sigma_D I_0\exp\left[-\rho_D t'-\left[g_D+\sum_{m=1}^{N_A}\delta_{nm}\right](t-t')\right]\ .$$

Therefore

$$\frac{\mathscr{D}(t)}{\Gamma_D \sigma_D I_0} = n_D \rho_D \int_0^t d\tau \exp\left[-\rho_D(t-\tau) - g_D\tau - \frac{4\pi}{3} n_A \sqrt{\pi \Delta \tau}\right] . \tag{9}$$

For the acceptors,

$$\mathscr{A}(t) = \frac{1}{V}\left\langle \Gamma_A \sum_{n=1}^{N_A} A_{1n} \right\rangle$$

and

$$\mathscr{A}(t) = \Gamma_A e^{-g_A t}\left[n_D \rho_D \sigma_D I_0 \left[\frac{e^{(g_A-\rho_D)t}-1}{g_A-\rho_D}\right] + n_A \rho_A \sigma_A I_0 \left[\frac{e^{(g_A-\rho_A)t}-1}{g_A-\rho_A}\right]\right]$$

$$-\frac{\Gamma_A}{\Gamma_D}(g_D-\rho_D)\int_0^t dt' e^{-g_A(t-t')}\mathscr{D}(t') - \Gamma_A n_D \rho_D \sigma_D I_0 e^{-g_A t}\int_0^t dt' \exp\left[g_A-g_D)t' - \frac{4\pi}{3} n_A \sqrt{\pi \Delta t'}\right] , \tag{10}$$

where $n_D = N_D/V$ = number of donors per unit volume, $n_A = N_A/V$ = number of acceptors per unit volume, and $\Delta = 1/\tau_D (R_0/R)^6$.

Substituting $\mathscr{D}(t')$ into $\mathscr{A}(t)$, we obtain

$$\frac{\mathscr{A}(t)}{\Gamma_A \sigma_A I_0} = \left[n_D \rho_D \beta \frac{(e^{-\rho_D t} - e^{-g_A t})}{g_A - \rho_D} + n_A \rho_A \frac{(e^{-\rho_A t} - e^{-g_A t})}{g_A - \rho_A}\right]$$

$$-\left[\frac{g_D-\rho_D}{g_A-\rho_D}\right] n_D \rho_D \beta e^{-\rho_D t}\int_0^t d\tau \exp\left[(\rho_D - g_D)\tau - \frac{4\pi}{3} n_A \sqrt{\pi \Delta \tau}\right]$$

$$+\left[\frac{g_D-\rho_D}{g_A-\rho_D}\right] n_D \rho_D \beta e^{-g_A t}\int_0^t d\tau \exp\left[(g_A - g_D)\tau - \frac{4\pi}{3} n_A \sqrt{\pi \Delta \tau}\right]$$

$$-n_D \rho_D \beta e^{-g_A t}\int_0^t d\tau \exp\left[(g_A - g_D)\tau - \frac{4\pi}{3} n_A \sqrt{\pi \Delta \tau}\right] , \tag{11}$$

where $\beta = \sigma_D/\sigma_A$ is the ratio of absorption cross sections of the donor and acceptor, g_D^{-1} = fluorescence decay time of the donor in a neat solution, and g_A^{-1} = fluorescence decay time of the acceptor in a neat solution. Varying the parameters R_0, β, g_D, and g_A, we have calculated the fluorescence per unit volume versus time for donor and acceptor molecules using Eqs. (9) and (11).

Standard numerical computer analysis was used to solve Eqs. (9) and (11). The results are shown in Figs. 3, 4, 5, and 6. The calculations for different parameters will be described in the next subsections.

For a neat solution the fluorescence intensity profile versus time is described by the equation

$$F(t) = \frac{\rho_F}{\rho_F - g_F}(e^{-g_F t} - e^{-\rho_F t}) , \tag{12}$$

where ρ_F = vibrational relaxation rate, and g_F^{-1} = fluorescence decay time. Using Eq. (12) the calculated fluorescence profile of neat solution rhodamine B and nile-blue-A-perchlorate are shown in Figs. 7 and 8, respectively. Comparing Figs. 7 (neat) and 3(a) (mixture), we observe a faster decay

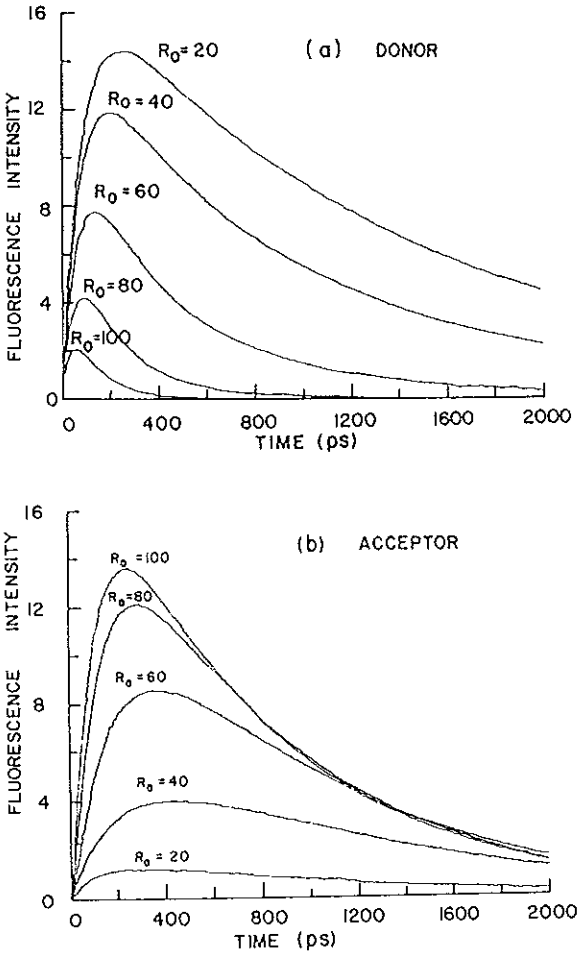

FIG. 3. Theoretical calculation of fluorescence profile versus time obtained by Eqs. (9) and (11) for (a) donor and (b) acceptor for various $R_0=20$, 40, 60, 80, and 100 Å. The detection system rise time is assumed to be 80 ps, considering the resolution of streak camera. The fluorescence decay time is assumed to be 1.5 and 0.75 ns for donor and acceptor, respectively. The ratio of absorption coefficient of donor to acceptor is 17.5. The concentration is $2.5\times10^{-3}M$.

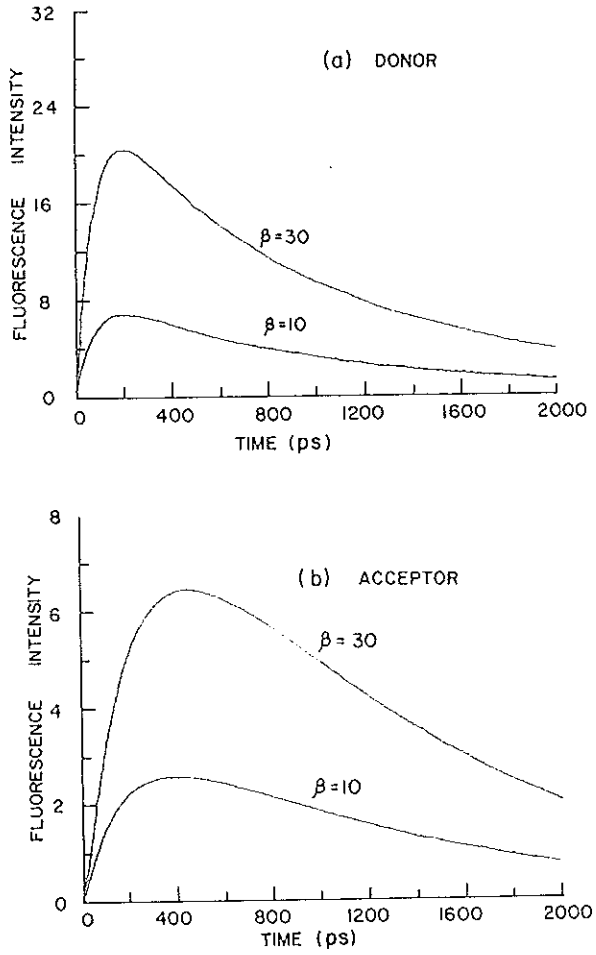

FIG. 4. Theoretical calculation of fluorescence profile versus time obtained by Eqs. (9) and (11) for (a) donor and (b) acceptor for different ratios of absorption of donor and acceptor, $\beta=30$ and 10. The detection rise time is 80 ps. The fluorescence decay time is assumed to be 1.5 and 0.75 ns for donor and acceptor, respectively. The concentration is $2.5\times10^{-3}M$ and $R_0=40$ Å.

kinetics for rhodamine *B* in the mixed solution than in neat solution. Both curves have fast rise times. Comparing Figs. 8 and 3(b), we observe a much slower rise of fluorescence for nile-blue-*A*-perchlorate in the mixed solution than in the neat solution. These results give information for the theoretical description of the behavior of the energy transfer from rhodamine *B* (the donor) to the nile-blue-*A*-perchlorate (the acceptor).

The numerical solutions for the various parameters R_0, β, g_D, and g_A on the fluorescence kinetics profile of donor and acceptor molecules are discussed in the following four subsections.

A. R_0 variation

The parameter R_0 was varied from 20 Å to 100 Å for the calculation of the fluorescence of donor and acceptor molecules. These results are shown in Figs. 3(a) and 3(b). The other parameters such as P_D, P_A, g_D, g_A, and β in the Eqs. (9) and (11) remain fixed. The values of the parameters are given in the figure caption of Fig. 3. In Fig. 3(a), for a given concentration of molecules (2.5×10^{-3} *M*, gives $\bar{R}^{DA}=43.5$ Å, $\bar{R}^{DD}=\bar{R}^{AA}=54$ Å, the peak intensity of donor fluorescence decreases as R_0 increases indicating more energy transfer. In Fig. 3(b), the peak intensity of the acceptor increases and the rise time becomes faster as R_0 in-

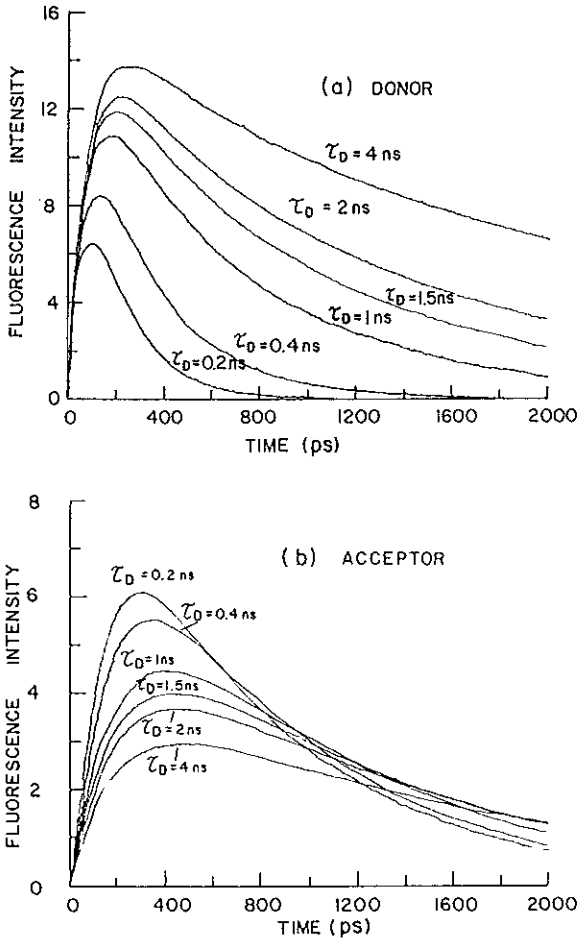

FIG. 5. Theoretical calculation of fluorescence profile versus time obtained by Eqs. (9) and (11) for (a) donor and (b) acceptor for different fluorescence decay times of donor τ_D (4, 2, 1.5, 1, 0.4, 0.2 ns). The detection system rise time is 80 ps. The fluorescence decay time is 0.75 ns for the acceptor. The concentration is $2.5\times10^{-3}M$ and the ratio of absorption coefficient is 17.5, and $R_0=40$ Å.

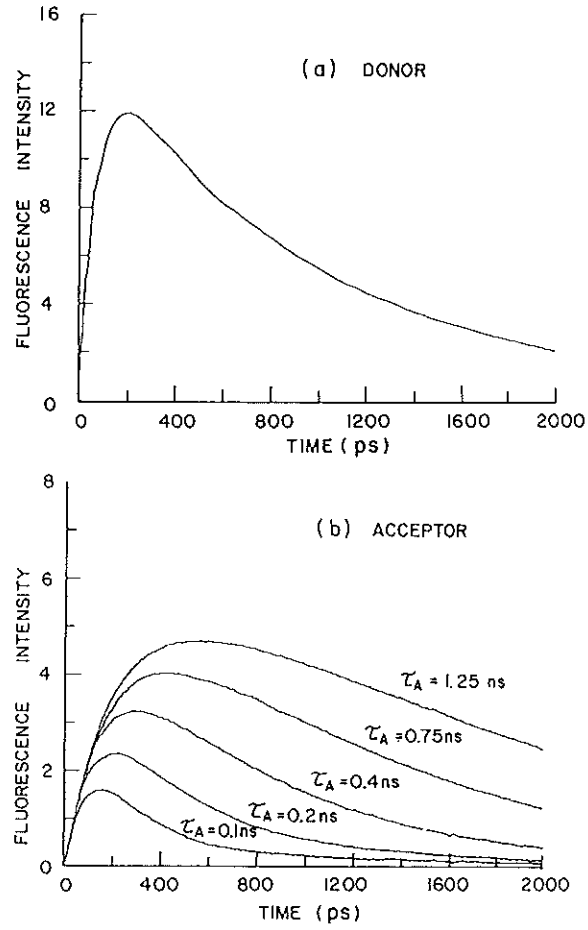

FIG. 6. Theoretical calculation of fluorescence profile versus time obtained by Eqs. (9) and (11) for (a) donor and (b) acceptor for different fluorescence decay times of acceptor τ_A (1.25, 0.75, 0.4, 0.2, 0.1 ns). The detection rise time is 80 ps. The fluorescence decay time is 1.5 ns for the donor. The concentration is $2.5\times10^{-3}M$. The ratio of absorption coefficient is 17.5, and $R_0=40$ Å. The fluorescence decay time of the donor $\tau_D=1.5$ ns.

creases. Physically, this means the energy transfer is more efficient if the separation distance R between the donor and acceptor molecules for a given concentration is less than R_0. If R_0 increases continuously, the energy transfer becomes so efficient that the donor acts like a pumping laser pulse which provides the energy. The intensity of the fluorescence profile of the acceptor abruptly increases because of a much higher-energy absorption ability of the donor, which provides almost all of the energy it absorbed to the acceptor. In this case, the acceptor fluoresces in the same way as though it was pumped directly by a laser pulse in a neat solution (actually, it gained energy from the donor). So, the rise time of the acceptor looks very

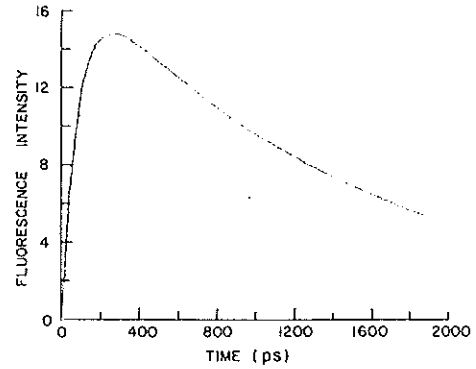

FIG. 7. Theoretical calculation of fluorescence profile versus time obtained by Eq. (12) for a donor in neat solution. The detection system rise time is 80 ps and the fluorescence decay time is 1.5 ns.

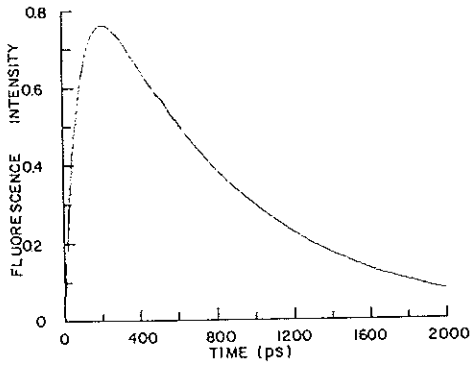

FIG. 8. Theoretical calculation of fluorescence profile versus time obtained by Eq. (12) for an acceptor in neat solution. The detection system rise time is 80 ps and the fluorescence decay time is 0.75 ns.

much like that in the neat solution and we observe the time displacement between the peak and the starting point of the fluorescence profile becomes smaller as R_0 reaches 100 Å.

B. Ratio of donor and acceptor absorption cross section β

The ratio β of the absorption cross section of the donor to that of the acceptor was varied from 10 to 30. The fluorescence of the donor and the acceptor for different values of β are shown in Figs. 4(a) and 4(b), respectively. The value of β defines the ratio of the amount of energy of the incident laser pulse absorbed directly by the donor and acceptor. A large value of β indicates a smaller absorption by the acceptor. The acceptors are chosen such that the direct absorption ability of laser energy is much weaker than the donor. In our case, the fluorescence from the acceptors occurs from the optically excited donors via energy transfer. Thus, the fluorescence kinetics depends on the energy transfer from the donor to the acceptor for large values of β.

C. Effect of the donor fluorescence decay time: τ_D

By changing the value of the donor decay time, the fluorescence kinetics profiles of the donor and acceptor are calculated in Figs. 5(a) and 5(b). The fluorescence decay time of acceptor τ_A for this calculation is fixed at 0.75 ns. In the neat donor solution, the longer the fluorescence decay time, the larger the fluorescence quantum yield and more light is emitted. In the binary dye mixture, as the fluorescence decay time increases, the fluorescence intensity of the donor molecules increases. In this case, the resonant energy transfer through the dipole-dipole interaction is decreased because energy is spread out over a larger time interval (transfer rate $\sim 1/\tau_D$). Therefore, the fluorescence intensity of the acceptor decreases in the low-energy transfer case when the fluorescence decay time of the donor molecule increases.

D. Effect of acceptor fluorescence decay time: τ_A

The calculated kinetic profiles of the acceptor molecule in the dye mixtures are shown in Fig. 6 for different fluorescence decay times of the accep-

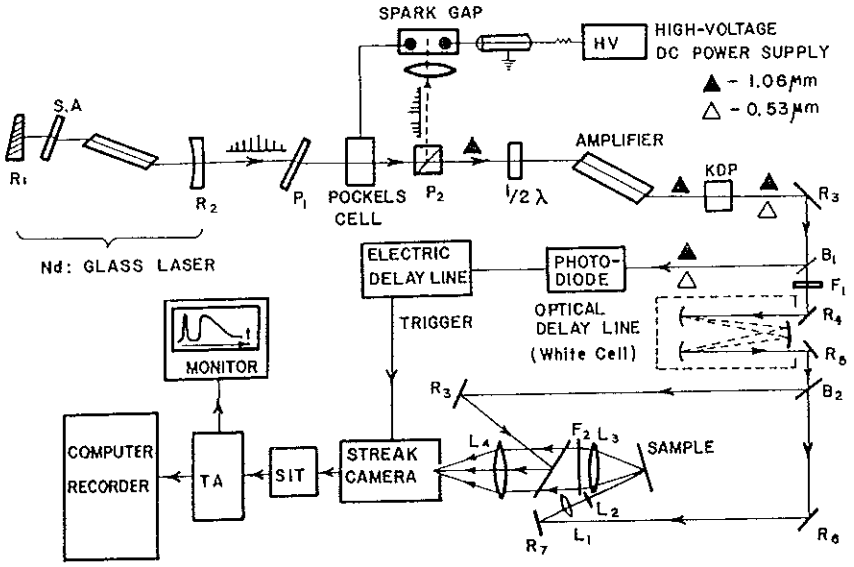

FIG. 9. Schematic diagram of the time-resolved fluorescence experimental setup.

tor molecule. The donor decay time is fixed at 1.5 ns. These results show that the acceptor molecule excited by energy transfer from the donor fluoresces with complex behavior. The acceptor molecules are excited by resonant dipole-dipole interaction and then fluorescence. So, the longer the fluorescence decay time, the slower the decay of the acceptor in the mixture solution. As expected, there is little effect on the fluorescence kinetics of the donor in the mixture for different fluorescence decay times of the acceptor.

III. EXPERIMENTAL SETUP

The experimental setup[21] used in this research program is shown in Fig. 9. The 1.054-μm laser beam is generated by the Nd:phosphate glass oscillator and amplifier. The single pulse selector is used to select a single pulse from the mode-locked pulse train. A second harmonic generator, potasium dihydrogen phosphate (KDP) converts the frequency of the 1.054 to 0.527 μm.

The 0.527-μm single pulse is delayed by an optical delay unit (White cell), and incident onto the sample. The excitation pulse is filtered by a Corning filter 3-67 from the fluorescence from the sample. A cyan dichroic filter is used to separate the fluorescence component of rhodamine 6*G*, and Hoya R-66 filter is used for the component of oxazine-4-perchlorate. The Ditric short pass filter at 620 nm is used to separate the fluorescence component of rhodomine *B*, and the Hoya R-68

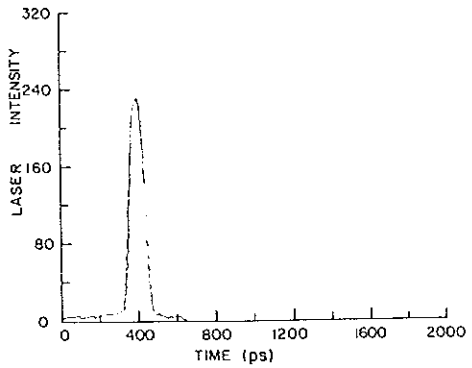

FIG. 10. Time response of the streak camera system on a 3-ns sweep scale—a 6 ps, 530-nm laser pulse profile versus time measured by streak camera system. This is the time convolution of the laser pulse and the system function of the detection apparatus. The pulse width at half maximum is about 80 ps. This is the time response function of the detection system on the streak rate used (3.1 ns full-time display).

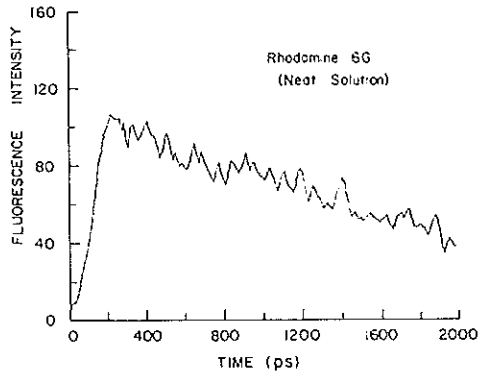

FIG. 11. Experimental measurement of fluorescence profile versus time of neat rhodamine 6*G* in ethylene glycol at a concentration $2.5\times10^{-3}M$. Using Corning 3-67 filters and a cyan dichroic filter, the fluorescence decay time is found to be 1.8 ns$\pm$0.15 ns (5300 Å $<\lambda<$ 6000 Å) by least-squares data fitting.

filter is used for the component of nile-blue-*A*-perchlorate. The fluorescence is collected by lenses and focused into the slit Hamamatsu streak camera[22] (C 979). The streak camera has a time resolution of $\lesssim$10 ps on the fastest sweep range of a 400-ps total time display. The streak camera output is recorded and digitized by a silicon intensified target (SIT) camera and Hamamatsu Temporal Analyzer. The data are stored and corrected for streak rate and intensity by Digital Minc 11 minicomputer. On the full-time display of 3.1 ns, the overall resolution of streak camera at this streak rate for these measurements is 80 ps. The system response for a laser pulse (pulse duration $=$6 ps measured by two photon fluorescence technique) is shown in Fig. 10. The system time response at full

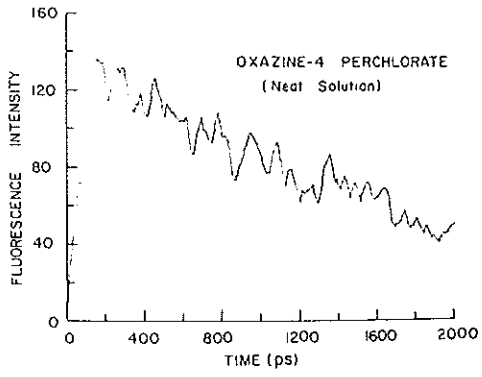

FIG. 12. Experimental measurement of fluorescence profile versus time of neat oxazine-4-perchlorate in ethylene glycol with a concentration $2.5\times10^{-3}M$. Using Corning 3-67 filters and Hoya R-66 filter, the fluorescence decay time is found to be 1.52 ns$\pm$0.1 ns ($\lambda>$ 6600 Å) by least-squares data fitting.

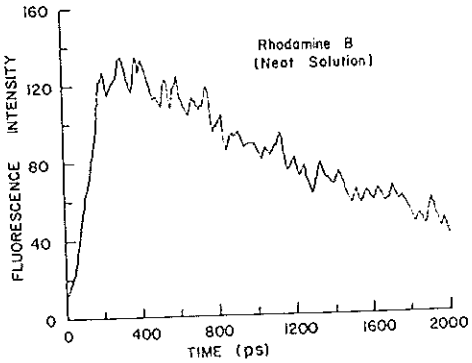

FIG. 13. Experimental measurement of fluorescence profile versus time of neat rhodamine B in ethylene glycol with a concentration $2.5\times10^{-3}M$. Using 3-67 filters and Ditric short pass filter at 620 nm, the fluorescence decay time is found to be 1.5 ns$\pm$0.16 ns (5300 Å $<\lambda<$ 6200 Å) by least-squares data fitting.

width at half maximum power is around 80 ps for the convolution of the laser pulse signal with the system function in time on the 3.1 ns full scale. Only the 2-ns part of the total display is displayed in Fig. 10. A portion of the excitation pulse is directed into the streak camera as a marker prepulse. The absolute zero time point for the fluorescence is determined by measuring the time period between the prepulse and the scattered excitation light from the surface of the sample. The streak camera is focused for spectral region from 530 to 750 nm.

The laser-grade dye samples (Eastman Kodak Company) was dissolved in the certified ethylene glycol (Fisher Scientific Company). A concentration of $2.5\times10^{-3}M$ for both the neat (similar, monocomponent system) and binary mixture (dissimilar, two-component system) solution was prepared. At this concentration the average distance $\bar{R}$ between the donor and acceptor molecules is about 43.5 Å, and the average distance between donor-donor molecules in the mixture is 54 Å. The solution was contained in a 1- or 2-mm optical path cuvette. The ratio of absorption coefficient β at $\lambda=530$ nm for rhodamine $6G$ to that of oxazine-4-perchlorate, and rhodamine B to that of nile-blue-A-perchlorate was measured to be 22 and 17.5, respectively. At these absorption ratios, very little direct pumping of the acceptor molecules is possible in the mixed system.

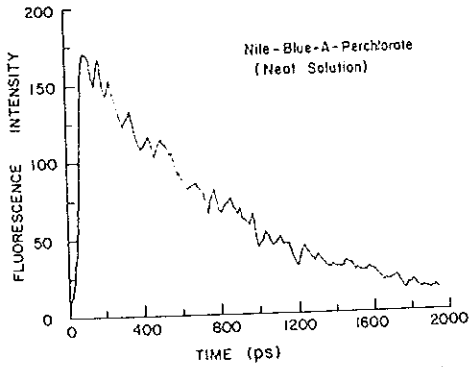

FIG. 14. Experimental measurement of the fluorescence profile versus time of neat nile-blue-A-perchlorate in ethylene glycol with a concentration $2.5\times10^{-3}M$. Using Corning 3-67 and Hoya R-68 filters, the fluorescence decay time is found to be 0.75 ns$\pm$0.05 ns ($\lambda>6800$ Å) by least-squares data fitting.

IV. EXPERIMENTAL RESULTS

A. Neat sample kinetics

The fluorescence kinetic from neat monocomponent solutions of dyes of rhodamine $6G$, oxazine-4-perchlorate, rhodamine B, and nile-blue-A-perchlorate in neat solution are shown in Figs. 11, 12, 13, and 14, respectively. The rise time of fluorescence is the time convolution of the system response function (80 ps) of our detection system on the 3.1-ns full-time scale. The fluorescence decay time is determined by a least-square single exponential data fitting. The decay times are 1.8,

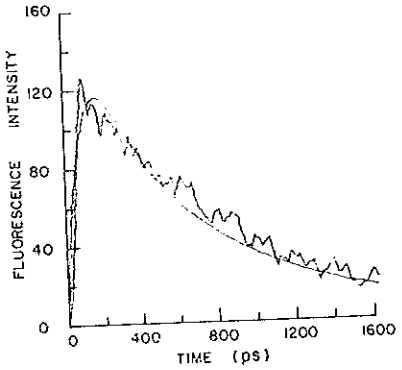

FIG. 15. Experimental measurement of fluorescence profile versus time of rhodamine $6G$ (the donor) mixed with oxazine-4-perchlorate (the acceptor) in ethylene glycol with a single concentration of $2.5\times10^{-3}M$. (5300 Å $<\lambda<$ 6000 Å). The filters used are Corning 3-67 and cyan dichroic filters. The measurement is fitted by a solid curve generated theoretically from Eq. (9). The parameters used to fit the donor data are the system rise time of 80 ps, the fluorescence decay time of 1.8 and 1.52 ns for the donor and acceptor molecules, respectively, the ratio of absorption coefficient of the donor and acceptor of 22, and value $R_0=55$ Å.

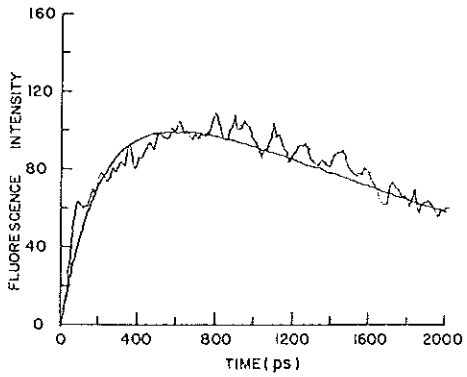

FIG. 16. Experimental measurement of fluorescence profile versus time of oxazine-4-perchlorate (the acceptor) mixed with rhodamine 6*G* (the donor) in ethylene glycol with a single concentration of $2.5\times10^{-3}M$ ($\lambda>6600$ Å). The filters used are Corning 3-67 and Hoya R-66 filters. The measurement is fitted by a solid curve generated theoretically from Eq. (11). The parameters used to fit the acceptor data are the system response of 80 ps, the fluorescence decay time of 1.8 and 1.52 ns for the donor and acceptor, respectively, the ratio of absorption coefficient of donor and acceptor of 22, and value $R_0=55$ Å.

1.52, 1.5, and 0.75 ns at $C=2.5\times10^{-3}$ M for Figs. 11 (R6*G*), 12 (OX), 13 (R*B*), and 14 (NB), respectively. The standard error for these decay times is ≤0.2 ns.

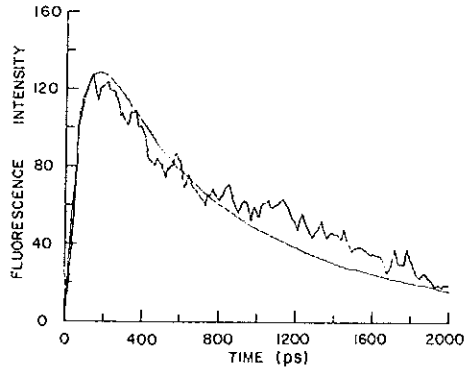

FIG. 17. Experimental measurement of fluorescence profile versus time of rhodamine *B* (the donor) mixed with nile-blue-*A*-perchlorate in ethylene glycol with single concentration of $2.5\times10^{-3}M$ (5300 Å $<\lambda<$ 6200 Å). The filters used are Corning 3-67 and Ditric short pass filter at 620 nm. The measurement is fitted by a solid curve generated theoretically from Eq. (9). The parameters used to fit the donor data are the system rise time of 80 ps, the fluorescence decay time of 1.5 and 0.75 ns for donor and acceptor, respectively, the ratio of absorption coefficient of donor and acceptor of 17.5, and value $R_0=48$ Å.

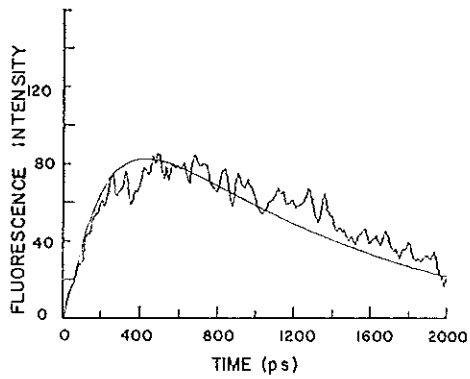

FIG. 18. Experimental measurement of fluorescence profile versus time of nile-blue-*A*-perchlorate (the acceptor) mixed with rhodamine *B* (the donor) in ethylene glycol with a single concentration of $2.5\times10^{-3}M$ ($\lambda>6800$ Å). The filters used are Corning 3-67 and Hoya R-68 filters. The measurement is fitted by a solid curve generated theoretically from Eq. (11). The parameters used to fit the acceptor data are the system rise time of 80 ps, the fluorescence decay time of 1.5 and 0.75 ns for the donor and acceptor, respectively, the ratio of absorption coefficient of 17.5, and value of R_0 =48Å.

B. Donor-acceptor mixture kinetics

The fluorescence of rhodamine 6*G* (the donor) and oxazine-4-perchlorate (the acceptor system; and rhodamine *B* (the donor) and nile-blue-*A*-perchlorate (the acceptor) system are shown in Figs. 15, 16, 17, and 18, respectively.

From Figs. 15 and 10, we found that $1/e$ time of the donor in the mixture becomes shorter compared to the fluorescence decay time of the donor molecule in the neat solution. The shortening is about 700 and 200 ps for rhodamine 6*G* and rhodamine *B*, respectively. From Figs. 16 and 12, we found that the rise time of the acceptor in the binary mixture becomes slower compared to that of the neat solution. The measured rise time is 650 and 400 ps slower than neat oxazine-4-perchlorate and neat nile-blue-*A*-perchlorate of 80 ps (system time resolution), respectively. This is attrubuted to the energy transfer from the donor to the acceptor because the rate of energy transfer to the excited state of the acceptor molecule is much slower than the feeding rate by vibrational relaxation.

V. DISCUSSION

The experimental fluorescence kinetics profiles of both the donor and acceptor were fitted by sub-

situting the experimental value of P_D, g_D, P_A, g_A, and β in Eqs. (9) and (11) for a different value of R_0. The experimental results of the donor and acceptor can be fitted very well with an appropriate value of R_0. This is a one-parameter fit (R_0). The parameter R_0 for the best fit to the data for (1) the mixture of rhodamine 6*G* and oxazine-4-perchlorate system is 55 Å$\pm$1 Å, and (2) rhodamine *B* and nile-blue-*A*-perchlorate system is 48 Å$\pm$2 Å.

We have performed the first measurement for fluorescence kinetics of both the donor and acceptor dye molecules and theoretically fitted the decay profiles of both the donor and the acceptor. The theory for the energy-transfer kinetics was developed to explain the change of decay of fluorescence of the donor, and the rise time of the fluorescence of the acceptor molecules. The theoretical fitting to the experimental kinetics profiles is excellent and consistent.

Theoretically, the parameter R_0 is the distance at which the rate of energy transfer is equal to the sum of all other donor deactivation rates. It can be expressed in terms of the overlapping integral of the emission spectrum of the donor and absorption spectrum of acceptor. The meaning of R_0 is just the strength of interaction between the donor and acceptor molecule. It is the distance parameter from which we can estimate if there is energy transfer, what concentration of solution we are able to make to get the efficient energy transfer. The values of R_0 were calculated[14] from spectroscopic data of fluorescence of the donor and absorption spectra: for R6*G*-OX 4, $R_0=56$ Å$\pm$1.1 Å and for R*B*-NB, $R_0=54$ Å$\pm$2 Å. These values are in excellent agreement with the values of R_0 obtained from fitting the time resolved measurements of donor and acceptor in this study. The values of R_0 are also in agreement with the results of Porter and Tredwell.[11] In addition, the critical transfer distance R_0^{DD} for donor-donor excitation transfer was calculated to be 41 and 40 Å for R6*G*-R6*G* and R*B*-R*B*, respectively. The donor-donor excitation transfer will occur at high concentration of donors[23] when the critical distance R_0^{DD} for *D-D* transfer is larger than the average distance $\bar{R}$ between molecules. The long-range energy-transfer rate between molecules decreases tremendously when the critical distance R_0 is less than the average distance $\bar{R}$ in the Förster mechanism. If $R_0 > \bar{R}$, there will be an increase in the long-range transfer. In order to enhance the energy transfer between donor and acceptor molecules, it is necessary to choose a pair of donors and acceptors such that (a) the absorption spectrum of the acceptor overlaps with the tail portion of the emission spectrum of the donor towards the longer-wavelength region as shown in Fig. 1; (b) the critical distance R_0^{DA} for donor-acceptor molecules is greater than that (R_0^{DD}) of donor-donor and $R_0^{DA} > \bar{R}^{DA}$, $\bar{R}^{DD} > R_0^{DD}$; (c) the absorption of laser energy by donors is high enough to overcome the absorption of laser energy by acceptors and to reduce the long-range *D-D* energy transfer to a minimum. In our cases the donor-donor energy transfer is not as important as donor-acceptor energy transfer because $R_0^{DA} > \bar{R}^{DA}$ and $\bar{R}^{DD} > R_0^{DD}$. If $R_0=0$, for instance, there is no overlapping of the emission spectrum of the donor and absorption spectrum of the acceptor. In this case, there is no energy transfer at all. This can be easily double checked by inserting $R_0=0$ in the Eqs. (9) and (11) to yield Eq. (12) immediately. The value of R_0 found for the rhodamine 6*G* and oxazine-4-perchlorate is larger than that of rhodamine *B* and nile-blue-*A*-perchlorate. These results give us another consistency check between the theory and experimental results.

Work is in progress for different concentrations of donor and acceptor molecules as well as a temperature dependence. This research will add more fundamental information on the mechanisms of energy transfer of *dyes in solutions and in glasses.*

ACKNOWLEDGMENTS

This research was supported by NSF Grant Energetics Engineering Program 7920192, NASA Grant No. NAG3130, and the City College Faculty Award Program. We thank Mr. P. Sekuler, Mr. A. Dagen, Dr. R. Seymour, and Dr. F. Pellegrino for technical assistance.

---

*Permanent address: Department of Physics, Zhongshan University, Canton, China.

[1]R. G. Bennett, J. Chem. Phys. 41, 3037 (1964).
[2]S. A. Latt, H. T. Cheung, and E. R. Blout, J. Am. Chem. Soc. 87, 995 (1965).
[3]K. B. Eisenthal, Chem. Phys. Lett. 6, 155 (1970).
[4]D. Rehm and K. B. Eisenthal, Chem. Phys. Lett. 9, 387 (1971).
[5]C. Lin and A. Dienes, J. Appl. Phys. 44, 5050 (1973).
[6]S. A. Ahmed, J. S. Gergely, and D. Infante, J. Chem.

Phys. 61, 1584 (1974).
[7]R. W. Anderson, Jr., R. M. Hochstrasser, H. Lutz, and G. W. Scott, J. Chem. Phys. 61, 2500 (1974).
[8]R. M. Hochstrasser and A. C. Nelson, Chem. Phys. Lett. 18, 361 (1976).
[9]R. Katraro, A. Ron, and S. Speiser, Chem. Phys. Lett. 52, 16 (1977).
[10]Yu, I. Bukekov, S. A. Tikhomirov, G. B. Tolstorozhev, and D. M. Khalimanovich, Sov. J. Quantum Electron. 7, 262 (1977).
[11]G. Porter and C. J. Tredwell, Chem. Phys. Lett. 56, 278 (1978).
[12]Th. Forster, Ann. Phys. (Leipzig) 2, 55 (1948); Discuss. Faraday Soc. 27, 7 (1959).
[13]K. B. Eisenthal and S. Siegel. J. Chem. Phys. 41, 652 (1964).
[14]J. B. Birks, *Photophysics of Aromatic Molecules* (Wiley, New York, 1970).
[15]R. G. Powell and Z. G. Soos, J. Lumin. 11, 1 (1975).
[16]D. L. Dexter, J. Chem. Phys. 21, 836 (1953).
[17]M. Yokota and O. Tanimoto, J. Phys. Soc. Jpn. 22, 779 (1967).
[18]U. K. A. Klein, R. Frey, M. Hauser, and U. Gosele, Chem. Phys. Lett. 41, 139 (1976).
[19]R. A. Auerbach, G. W. Robinson, and R. W. Zwanzig, J. Chem. Phys. 72, 3528 (1980).
[20]K. Allinger and A. Blumer, J. Chem. Phys. 72, 4608 (1980).
[21]P. Y. Lu, P. P. Ho, and R. R. Alfano, IEEE J. Quantum Electron. QE-15, 406 (1979).
[22]N. H. Schiller, Y. Tsuchiya, E. Inuzuka, Y. Suzuki, K. Kinoshita, K. Kamiya, H. Iida, and R. R. Alfano, Opt. Spectra 14, 55 (1980).
[23]D. P. Millar, R. J. Robbins, and A. H. Zewail, J. Chem. Phys. 75, 3649 (1981).